Aerospace Science and Technology 34 (2014) 84–91

Contents lists available at ScienceDirect

Aerospace Science and Technology

www.elsevier.com/locate/aescte

Influence of the startup and shutdown phases on the viscoplastic structural analysis of the thrust chamber wall

Jinhui Yang, Tao Chen, Ping Jin, Guobiao Cai *

School of Astronautics, BeiHang University, Beijing, 100191, PR China

ARTICLE INFO

Article history:
Received 13 December 2012
Received in revised form 27 August 2013
Accepted 9 September 2013
Available online 18 September 2013

Keywords:
Viscoplastic
Structural analysis
Life prediction
Startup phase
Shutdown phase

ABSTRACT

Detailed structural analysis with Robinson's viscoplastic model of the thrust chamber wall has been completed to explain its damage process phase by phase, indicating that under the same level of thermal–structure loadings, the startup and shutdown phases play an important role of the failure. Different startup and shutdown durations were applied to study the phase influence on structural analysis and predicted life. Results reveal that the startup process mainly affects the remaining strain, while the shutdown process contributes more to the remaining stress on the cyclic effect; quick startup and longer shutdown duration conduce to prolong the chamber life and the life can be promoted 22% through reducing start-up duration from 1.5 s to 0.3 s, while 5% through increasing shut-down duration from 0.15 s to 0.9 s.

1. Introduction

As one of the critical components of the reusable rocket engine, the thrust chamber is designed to operate in severe conditions of elevated temperature and pressure for improving the engine performance. At these elevated temperatures, in turn, the thrust chamber wall experiences significant inelastic strains. For an accurate estimation of the life of the chambers and to predict their progressive deformation with the number of loading cycles, a realistic stress–strain analysis must be made [8].

Unified viscoplastic analyses provide realistic descriptions of high-temperature inelastic behavior of materials, in which all inelastic strains (e.g. creep, plastic, relaxation, and their interactions) are accounted for as a single, time-dependent quantity. Arya and Arnold applied the Robinson's model [2] and Freed's model [1] to assess the inelastic deformation, which qualitatively replicated the doghouse effect, as shown in Fig. 1; Ray and Dai, basing on the Freed's viscoplastic model, captured the nonlinear effects to represent the inelastic strain ratcheting, progressive bulging out, and thinning in the thrust chamber wall, which contributed lots to the on-line service-life prediction and damage analysis of the thrust chamber [5]; Sung et al. applied conventional and viscoplastic models to predict a small scale experimental annular plug nozzle thruster life, and validated by cyclic test, which revealed that the viscoplastic model showed better agreement in predicting the life cycle failure when both low cycle fatigue and fatigue–creep interaction were taken into account [19,18]; Schwarz et al. developed a viscoplastic model including ageing that successfully captured the observed accrued thinning of the hot wall and quantitatively reproduced the doghouse deformation [17]. However, most of the previous researches focus on the final state analysis, while the damage process study phase by phase using the viscoplastic theory is blank.

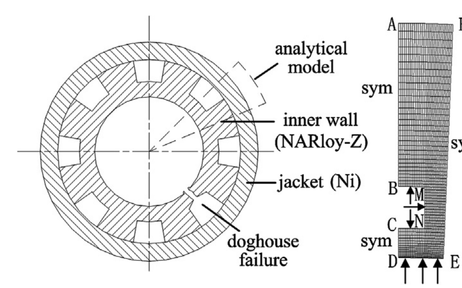

Fig. 1. Cross section sketch of thrust chamber and analytical model.

The thrust chamber used in experiments at the NASA Lewis Research Center was analyzed in this paper [11], which used NARloy-Z as inner wall and Ni as the jacket, as shown in Fig. 1. The right figure depicts the finite element model applied in the analysis. It consists of 2800 elements and 2941 nodes. The coupled thermal–mechanical plan strain solid elements were used to model the smallest repeating segment of the cylinder wall. Because the wall was symmetrical, only one-half of a cooling channel was modeled. Experimental results published by Quentmeyer [11,12] and Pavli [10] demonstrate that the crack initiates at point D (Fig. 1)

* Corresponding author. Tel.: +86 010 82336222; fax: +86 010 82338798.
E-mail address: cgb@buaa.edu.cn (G. Cai).

1270-9638/$ – see front matter
http://dx.doi.org/10.1016/j.ast.2013.09.004

Table 1
Cyclic thermal and pressure loadings.

Loadings	$h_{f,cool}$ kW/(K m^2)	T_{cool} K	P_{cool} MPa	$h_{f,cool}$ kW/(K m^2)	T_{hot} K	P_{hot} MPa
Precooling/post cooling	102	28	5.1	0	278	0.0965
Hot run	48.3	50	6.55	20.2	3364	2.78

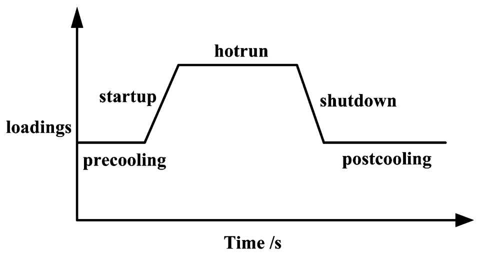

Fig. 2. Working phases and loading history.

of the inner wall, i.e. the "roof" point of the doghouse. In order to explain the damage process, detailed viscoplastic stress–strain analysis of point D was conducted in this paper. Due to considerable influence over the thrust chamber structural and life analysis exerted by the startup and shutdown phases, different durations of the two phases were studied in the paper. Our results show that quick startup and longer shutdown duration conduce to prolong the chamber life, which gives an improvement method for the reusable rocket engine.

2. Thermal–mechanical analysis models

2.1. Thermal analysis

Coupled thermal–mechanical analysis of the thrust chamber was completed under the boundary conditions [2] shown in Table 1 and Fig. 2. Five phases are taken into account as one working cycle: precooling, startup, hot run, shut-down and post cooling. Table 1 shows the cyclic loadings working on the coolant side and the hot gas side, which respectively represented by subscript "cool" and "hot". The convective film coefficient h_f and bulk temperature of the fluid T characterize the cyclic thermal loading, and P means the coolant and hot gas pressure.

The general heat equation for dynamic problems without internal heat sources is given as:

$$\rho c \frac{\partial T(x,t)}{\partial t} = -\operatorname{div} \lambda \nabla T(x,t) \quad (1)$$

where the ρ is density, c is specific heat, t is time and λ is thermal conductivity.

The thermal strain $\boldsymbol{\varepsilon}_{ij}^{th}$ is decided by the temperature increment:

$$\frac{\partial \boldsymbol{\varepsilon}_{ij}^{th}}{\partial t} = \alpha_{ij}(T)\frac{\partial T}{\partial t} \quad (2)$$

where $\alpha_{ij}(T)$ is the thermal expansion coefficient. Equivalent nodal forces are calculated from the thermal strain increment and then added to the nodal force vector for the solution of the problem.

2.2. Robinson's viscoplastic model

Robinson's model [16] employs a dissipation potential to derive the flow and evolutionary laws for the inelastic strain and internal state variables.

The total strain rate $\dot{\boldsymbol{\varepsilon}}_{ij}$ is decomposed into elastic $\dot{\boldsymbol{\varepsilon}}_{ij}^{el}$, inelastic $\dot{\boldsymbol{\varepsilon}}_{ij}^{in}$ (including plastic, creep, relaxation, etc.), and thermal $\dot{\boldsymbol{\varepsilon}}_{ij}^{th}$ strain rate components. Thus

$$\dot{\boldsymbol{\varepsilon}}_{ij} = \dot{\boldsymbol{\varepsilon}}_{ij}^{el} + \dot{\boldsymbol{\varepsilon}}_{ij}^{in} + \dot{\boldsymbol{\varepsilon}}_{ij}^{th} \quad (i,j=1,2,3) \quad (3)$$

The elastic strain rate for an isotropic material is governed by Hooke's law:

$$\dot{\boldsymbol{\varepsilon}}_{ij}^{el} = \frac{1+\nu}{E}\dot{\boldsymbol{\sigma}}_{ij} - \frac{\nu}{E}\dot{\boldsymbol{\sigma}}_{kk}\boldsymbol{\delta}_{ij} \quad (4)$$

where E is the Young's modulus, ν is the Poisson's ratio, and $\boldsymbol{\sigma}_{ij}$ is the stress. The repeated subscript in Eq. (4) and elsewhere implies summation over their range, and $\boldsymbol{\delta}_{ij}$ is the Kronecker delta function. A dot over a symbol denotes its derivative with respect to time t. The nonisothermal multiaxial inelastic constitutive equations for the model are given below:

Flow law:

$$\dot{\boldsymbol{\varepsilon}}_{ij}^{in} = \begin{cases} \frac{AF^n \boldsymbol{\Sigma}_{ij}}{\sqrt{J_2}} & F>0 \text{ and } \boldsymbol{S}_{ij}\boldsymbol{\Sigma}_{ij}>0 \\ 0F \leqslant 0 & \text{or } F>0 \text{ and } \boldsymbol{S}_{ij}\boldsymbol{\Sigma}_{ij} \leqslant 0 \end{cases} \quad (5)$$

Evolutionary law:

$$\dot{\boldsymbol{a}}_{ij} = \begin{cases} \frac{h}{G^\beta}\dot{\boldsymbol{\varepsilon}}_{ij}^{in} - \frac{rG^{m-\beta}}{\sqrt{I_2}}\boldsymbol{a}_{ij} & G<G_0 \text{ and } \boldsymbol{S}_{ij}\boldsymbol{a}_{ij}>0 \\ \frac{h}{G_0^\beta}\dot{\boldsymbol{\varepsilon}}_{ij}^{in} - \frac{rG_0^{m-\beta}}{\sqrt{I_2}}\boldsymbol{a}_{ij} & G \geqslant G_0 \text{ or } G<G_0 \text{ and } \boldsymbol{S}_{ij}\boldsymbol{a}_{ij}>0 \end{cases} \quad (6)$$

where

$$F = \frac{J_2}{K^2} - 1 \quad (7)$$

$$G = \frac{I_2}{K_0^2} \quad (8)$$

$$J_2 = \frac{1}{2}\boldsymbol{\Sigma}_{ij}\boldsymbol{\Sigma}_{ij} \quad (9)$$

$$I_2 = \frac{1}{2}\boldsymbol{a}_{ij}\boldsymbol{a}_{ij} \quad (10)$$

$$\boldsymbol{\Sigma}_{ij} = \boldsymbol{S}_{ij} - \boldsymbol{a}_{ij} \quad (11)$$

and

$$\left.\begin{aligned} \boldsymbol{S}_{ij} &= \boldsymbol{\sigma}_{ij} - \frac{1}{3}\boldsymbol{\sigma}_{kk}\boldsymbol{\delta}_{ij} \\ \boldsymbol{a}_{ij} &= \boldsymbol{\alpha}_{ij} - \frac{1}{3}\boldsymbol{\alpha}_{kk}\boldsymbol{\delta}_{ij} \end{aligned}\right\} \quad (12)$$

The material parameters for Robinson's model are taken from Ref. [2], which qualitatively replicated the "doghouse" effect and the thinning of the coolant channel wall. Effects of temperature are incorporated in the model through the temperature dependent parameters: Young's modulus E, hardening variable K, recovery or softening material parameter R and so on. Detailed viscoplastic stress–strain analysis of thrust chamber wall basing on the Robinson's model is conducted in the following section.

2.3. Uniformly valid asymptotic integration algorithm

Chulya and Walker present one uniformly valid asymptotic integration algorithm for the viscoplastic theory [4], which is implicit and has high stability and allows large time increments. By incorporating the algorithm into the finite element program MARC through a user subroutine called HYPELA2, a stress–strain analysis of the cylindrical thrust chamber wall was performed. Following